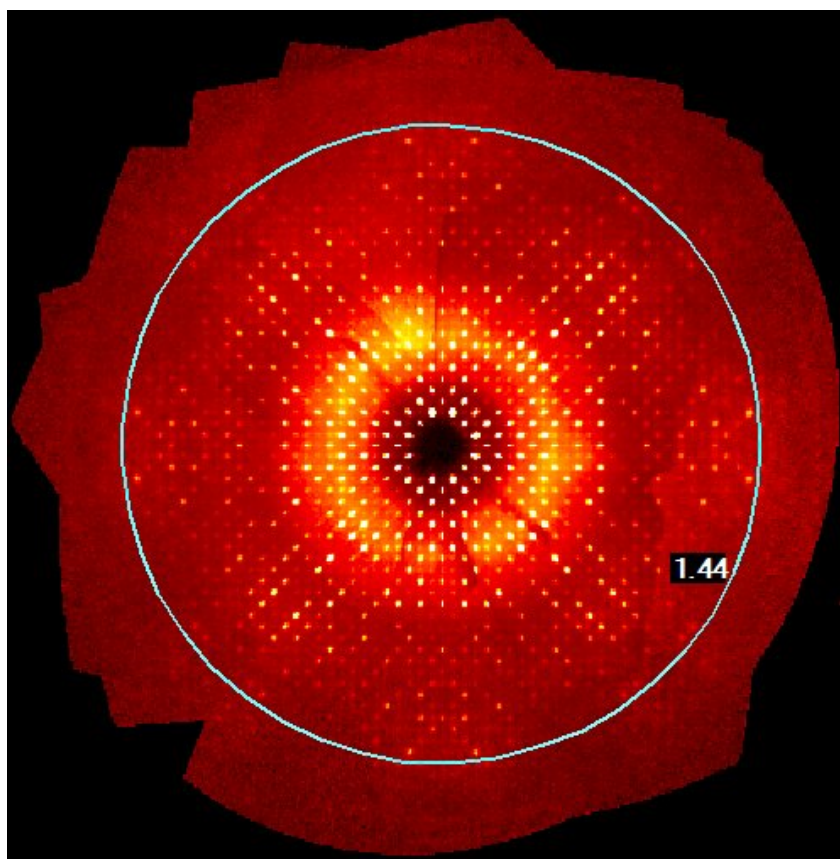


Supporting Information

Structure Modeling, Synthesis and X-Ray Diffraction Determination of an Extra-Large Calixarene-Based Coordination Cage and Its Application in Drug Delivery

Shangchao Du, Tang-Qing Yu, Wuping Liao* and Chunhua Hu*

1. Fig. S1. The precession image of the (h k 0) layer from CIAC-114.
2. Table S1. X-ray data collection details for CIAC-114.
3. The SQUEEZE result for CIAC-114.
4. Fig. S2. The connecting of one Co₄-SC4A-SO₂ subunit with four BBB ligands.
5. Fig. S3. Packing diagram of CIAC-114.
6. Fig. S4. SEM images for the activated samples and the Ibu-loaded samples.
7. Fig. S5. SEM images for H₄SC4A-SO₂ and H₄SC4A-SO₂ ⊃ Ibu.
8. Fig. S6. ESI-MS spectrum of CIAC-114.
9. Fig. S7. ¹H NMR spectra of CIAC-106 + Ibu.
10. Fig. S8. DOSY ¹H NMR spectra for CIAC-114 ⊃ Ibu in DMF.
11. Fig. S9. DOSY ¹H NMR spectra for Ibu in DMF.
12. Fig. S10. DOSY ¹H NMR spectra for CIAC-114 in DMF.
13. Fig. S11. ¹³C solid state NMR spectra of CIAC-106, CIAC-106 ⊃ Ibu.
14. Fig. S12. TGA-DSC curves for CIAC-114.
15. Fig. S13. TGA-DSC curves for CIAC-106 ⊃ Ibu.
16. Fig. S14. TGA-DSC curves for CIAC-114 ⊃ Ibu.
17. Fig. S15. TGA-DSC curves for H₄SC4A-SO₂ ⊃ Ibu.
18. Fig. S16. Chromatograms for the samples of CIAC-106 and CIAC-114 after immersed in PBS buffer solution for 22 hours.



1. Fig. S1. The precession image of the (h k 0) layer from **CIAC-114**.

2. Table S1. X-ray data collection details for CIAC-114.

| Axis | dx/mm | 2 θ / $^{\circ}$ | ω / $^{\circ}$ | φ / $^{\circ}$ | χ / $^{\circ}$ | Width/ $^{\circ}$ | Frames | Time/s | $\lambda/\text{\AA}$ | V/kV | Current/ mA | T/K |
|-------|--------|-------------------------|-----------------------|------------------------|---------------------|-------------------|--------|--------|----------------------|------|----------------|-----|
| Omega | 79.525 | -13.00 | 347.00 | 0.00 | 54.86 | -0.30 | 600 | 40.00 | 0.71073 | 50 | 36.0 | 120 |
| Omega | 79.525 | -13.00 | 347.00 | 90.00 | 54.86 | -0.30 | 600 | 40.00 | 0.71073 | 50 | 36.0 | 120 |
| Omega | 79.525 | -13.00 | 347.00 | 180.00 | 54.86 | -0.30 | 600 | 40.00 | 0.71073 | 50 | 36.0 | 120 |
| Omega | 79.525 | -13.00 | 347.00 | 270.00 | 54.86 | -0.30 | 600 | 40.00 | 0.71073 | 50 | 36.0 | 120 |
| Omega | 79.525 | -13.00 | 347.00 | 45.00 | 54.86 | -0.30 | 600 | 40.00 | 0.71073 | 50 | 36.0 | 120 |
| Omega | 79.525 | -13.00 | 347.00 | 135.00 | 54.86 | -0.30 | 600 | 40.00 | 0.71073 | 50 | 36.0 | 120 |
| Omega | 79.525 | -13.00 | 347.00 | 225.00 | 54.86 | -0.30 | 541* | 40.00 | 0.71073 | 50 | 36.0 | 120 |

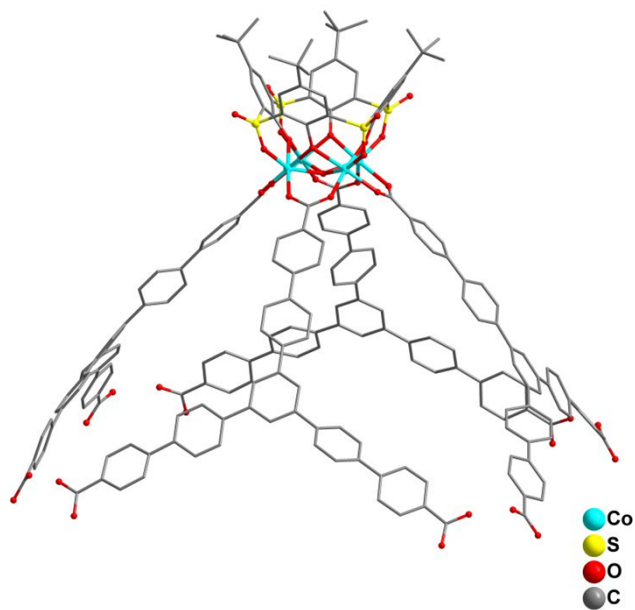
* We did not collect 600 frames for the last run. Since the data were enough, we stopped the data collection at our best convenience.

3. The SQUEEZE result for CIAC-114

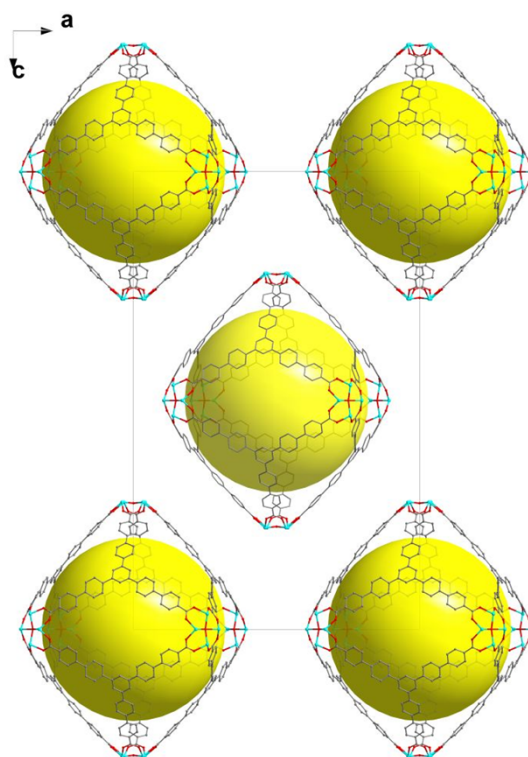
The cations and solvent molecules in the voids in and between the cages cannot be located from Difference Fourier maps, because they are disordered. Therefore, the data were treated by PLATON/SQUEEZE to estimate the contribution of these disordered groups.¹¹ The SQUEEZE output is listed below. The total 15626 electrons per unit cell were calculated, which are contributed by the disordered groups in the voids. There are two formula units per cell, so each unit has 7813 e⁻ for disordered cations and solvents. Of them 348 e⁻ account for six (C₂H₅)₃NH⁺ (C₆H₁₆N, 58 e⁻) as counter cations that balance the charge. The rest 7465 e⁻ correspond to about 156 N,N-dimethylacetamide (DMA, C₃H₇NO, 48 e⁻) molecules. So the appropriate chemical formula of **CIAC-114** is [(C₂H₅)₃NH]₆{[Co₄(SC4A-SO₂)(OH)]₆(BBB)₈}. 156(DMA), i.e. C₁₁₀₄H₁₈₁₈N₁₆₂O₂₈₂S₂₄Co₂₄.

loop_

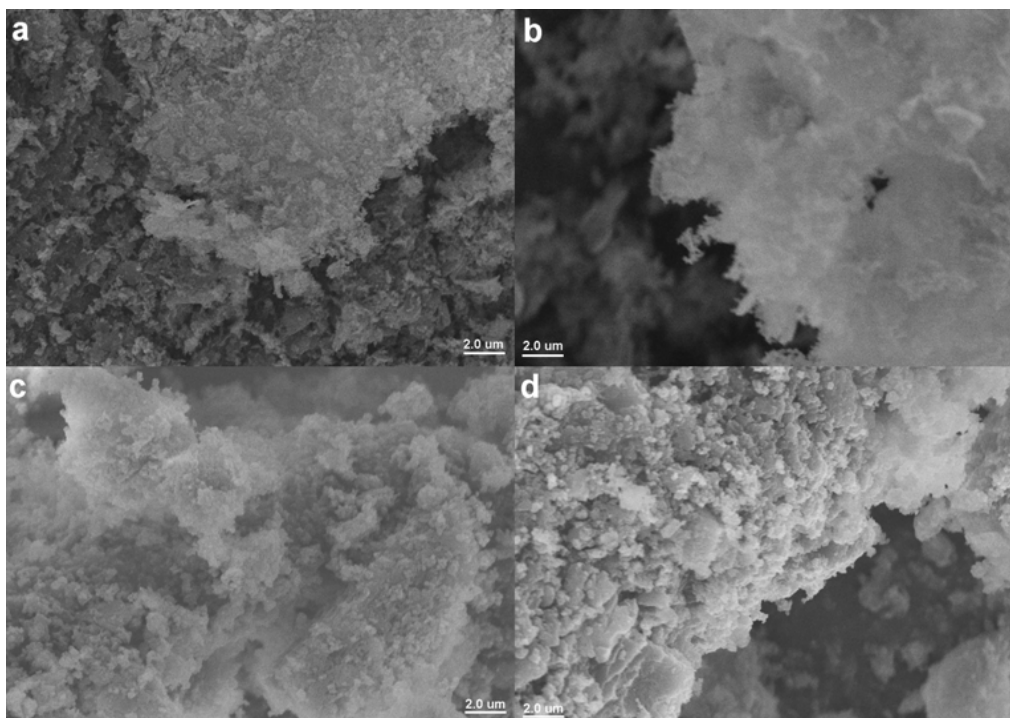
| _platon_squeeze_void_nr | _platon_squeeze_void_average_x | _platon_squeeze_void_average_y | _platon_squeeze_void_average_z | _platon_squeeze_void_volume | _platon_squeeze_void_count_electrons | _platon_squeeze_void_content |
|-------------------------|--------------------------------|--------------------------------|--------------------------------|-----------------------------|--------------------------------------|------------------------------|
| 1 | -0.002 | -0.010 | -0.002 | 83689 | 15102 | ' ' |
| 2 | 0.000 | 0.000 | 0.500 | 903 | 262 | ' ' |
| 3 | 0.500 | 0.500 | 0.000 | 903 | 262 | ' ' |



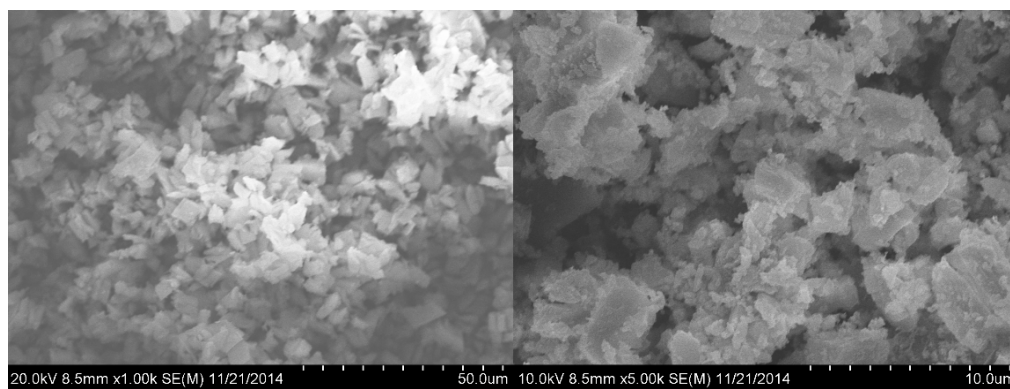
4. Fig. S2. The connecting of one Co₄-SC4A-SO₂ subunit with four BBB ligands.



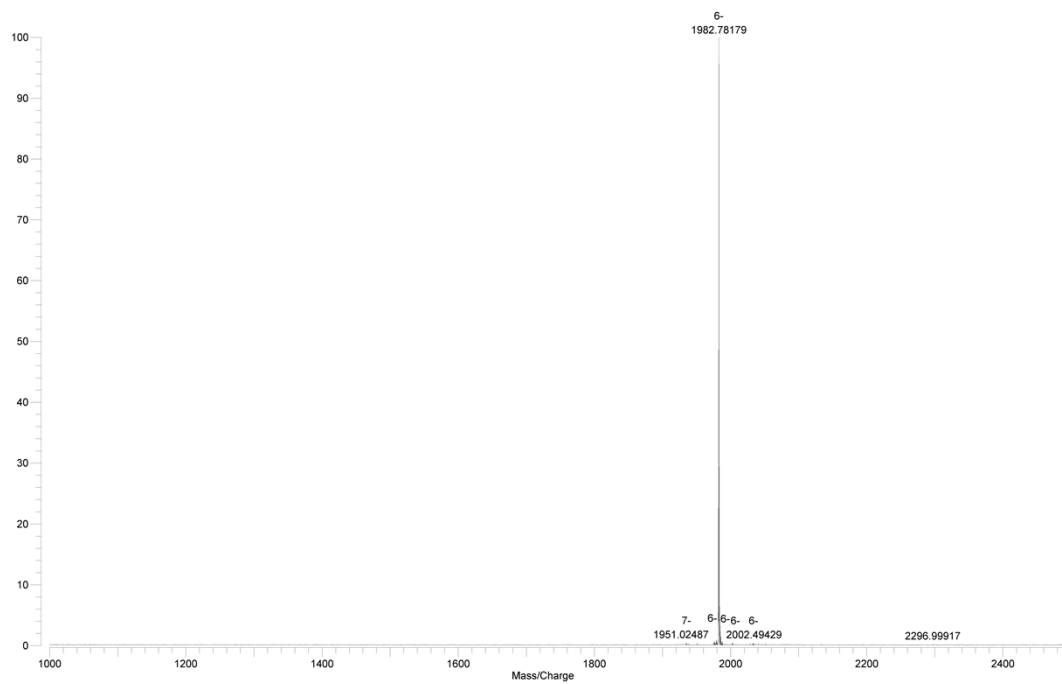
5. Fig. S3. Packing diagram of **CIAC-114**. The calixarene molecules are omitted for clarity.



6. Fig. S4. SEM images for the activated samples and the Ibu-loaded samples. (a) **CIAC-106**, (b) **CIAC-114**, (c) **CIAC-106**⊃Ibu and (d) **CIAC-114**⊃Ibu.

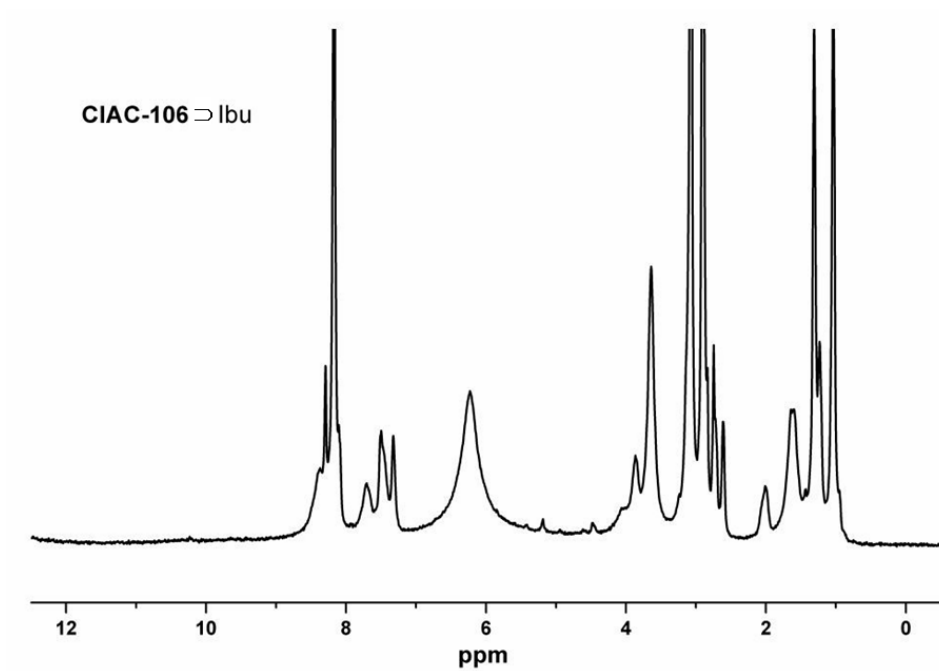


7. Fig. S5. SEM images for $H_4SC4A-SO_2$ (left) and $H_4SC4A-SO_2 \supset Ibu$ (right).

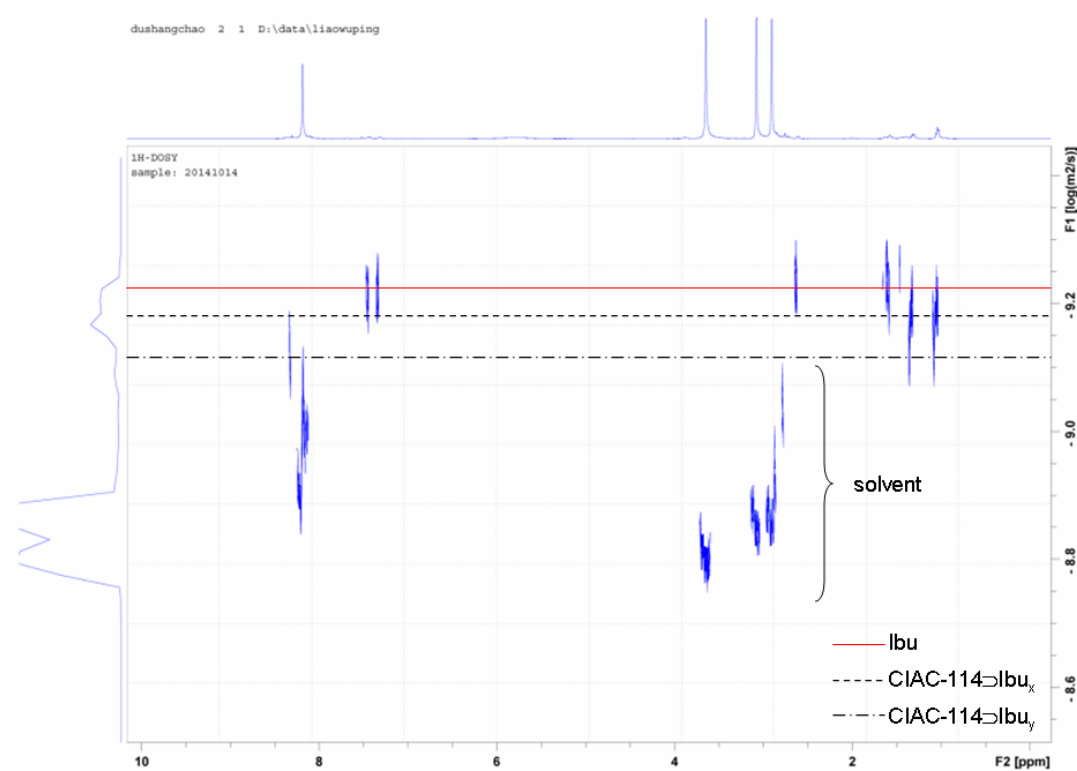


8. Fig. S6. ESI-MS spectrum of **CIAC-114** in a DMF-methanol mixture (1982.78:



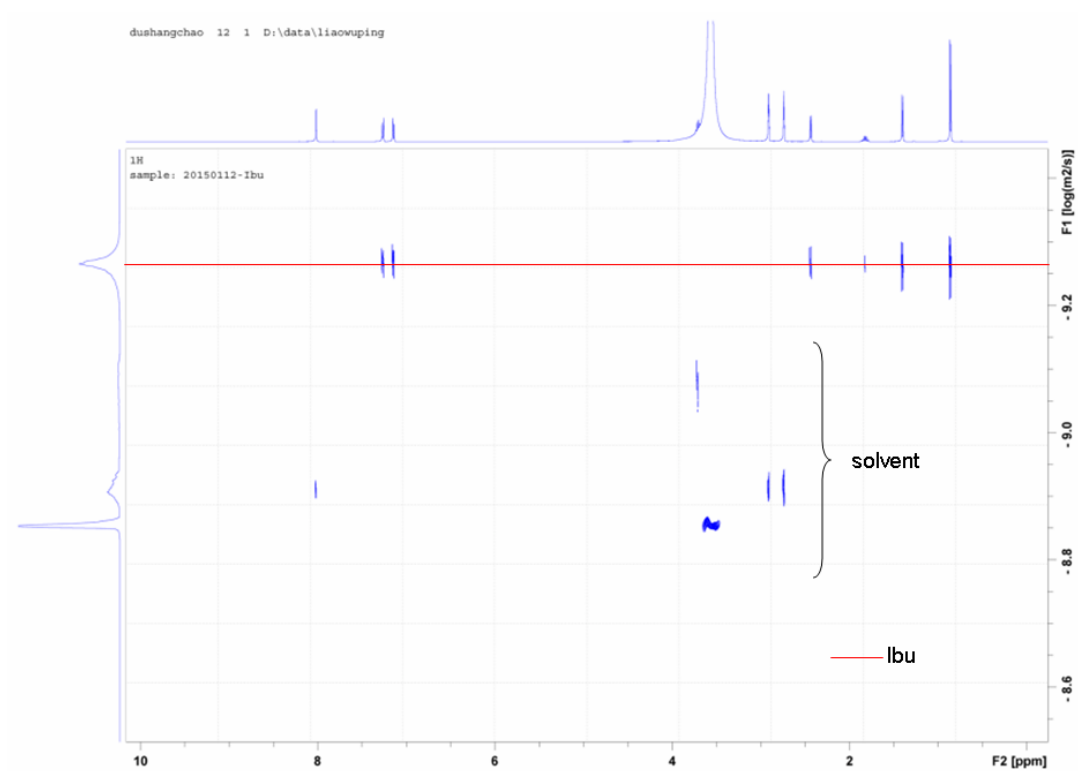


9. Fig. S7. ^1H NMR spectra of **CIAC-106** to Ibu.

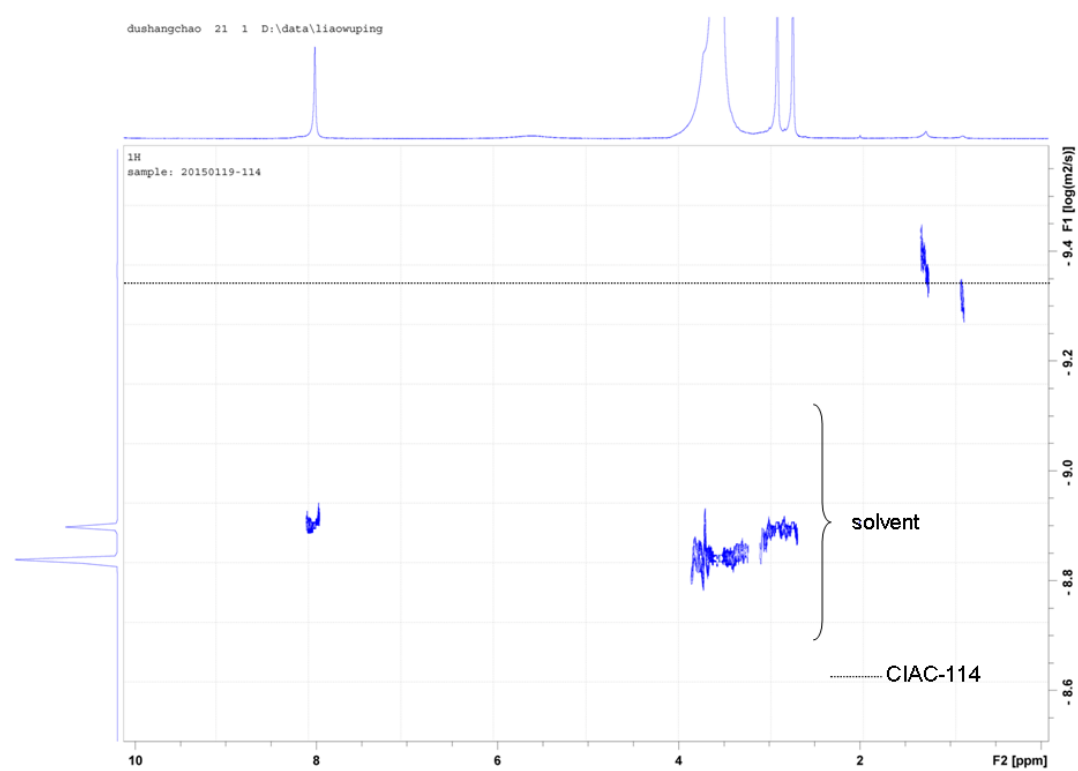


10. Fig. S8. DOSY ^1H NMR spectra for **CIAC-114**⊃Ibu in DMF.

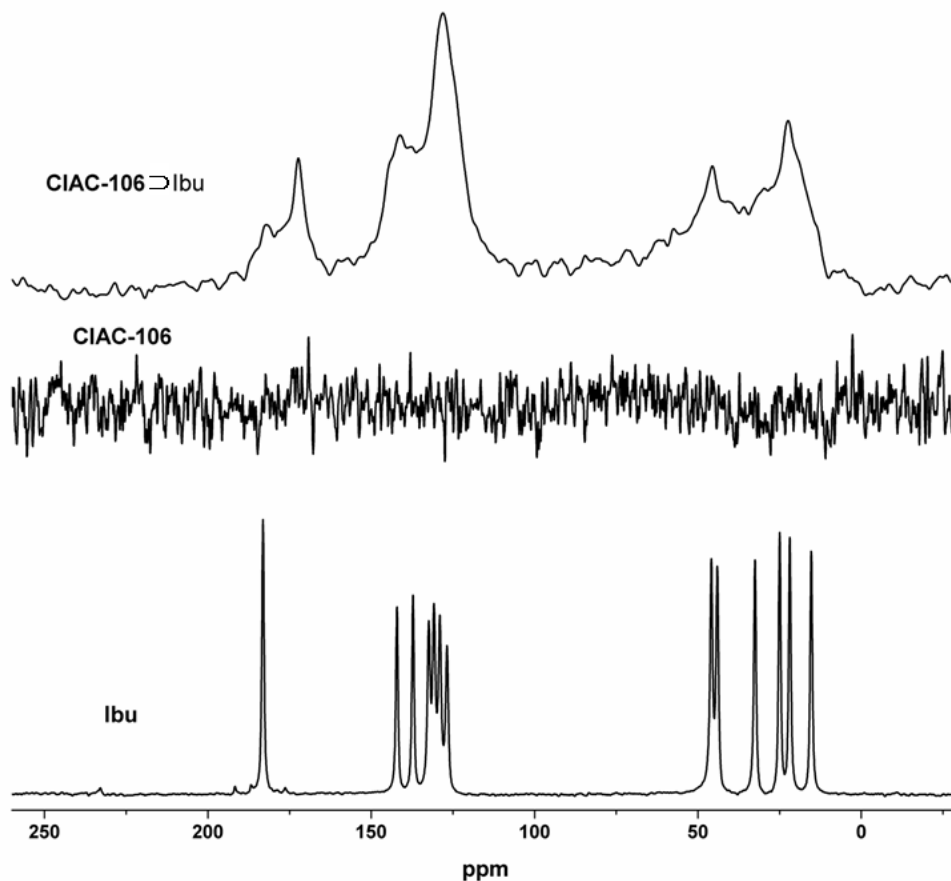
Diffusion-ordered (DOSY) NMR spectroscopy measurements for the samples of Ibu, **CIAC-114** and **CIAC-114**⊃Ibu in DMF were carried out (shown in Fig. S8-S10). Compared with the spectra for the pure Ibu and cage compound, the spectra of the loaded samples show chemical shifts of Ibu with nearly unchanged diffusion constant, which indicates some Ibu molecules are adhered to the cage structure by outer interactions. Furthermore, there are some chemical shifts with changed diffusion constant, which can be attributed to the guest-host structures of Ibu and **CIAC-114** in different ratio. It supports the fast release of Ibu at the first stage and slow release afterward.



11. Fig. S9. DOSY ¹H NMR spectra for Ibu in DMF.

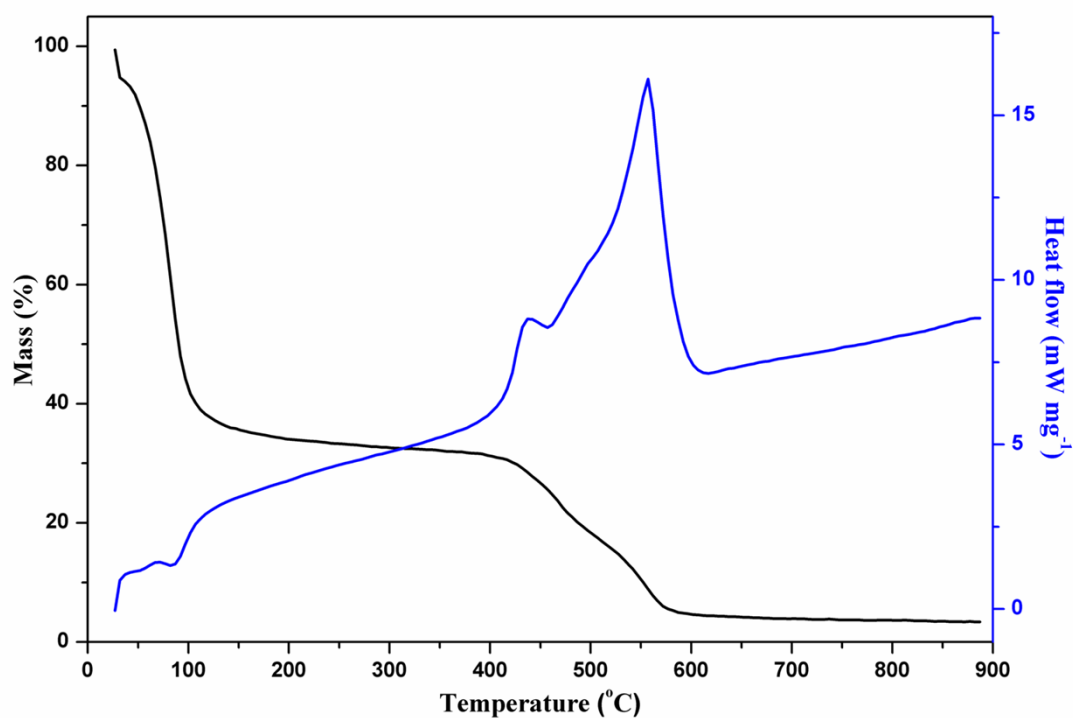


12. Fig. S10. DOSY ¹H NMR spectra for CIAC-114 in DMF.

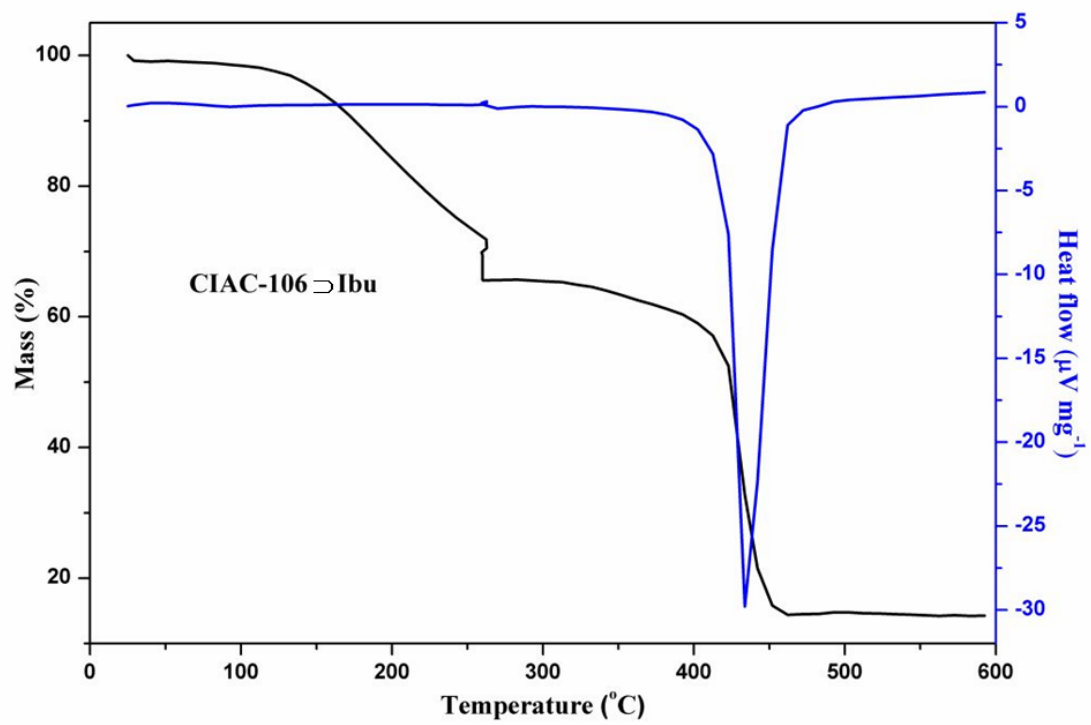


12. Fig. S11. ^{13}C solid state NMR spectra of Ibu, **CIAC-106** (activated samples), and **CIAC-106** \supset Ibu.

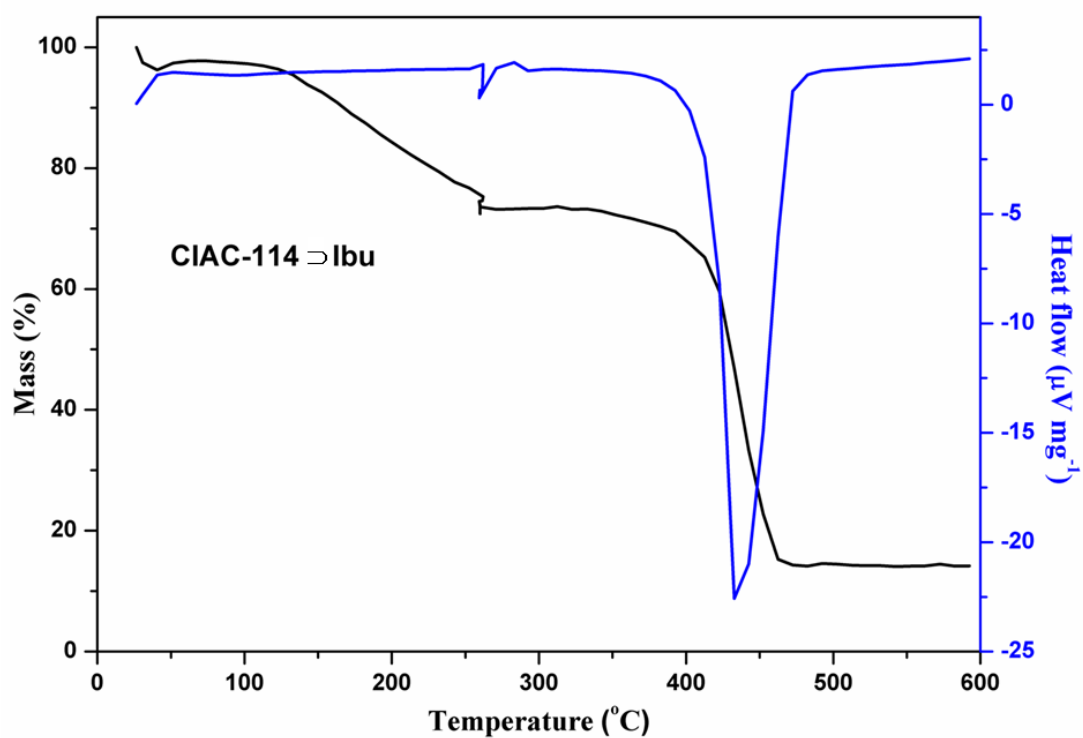
The ^{13}C solid state NMR experiments of Ibu, **CIAC-106** and **CIAC-106** \supset Ibu were carried out. The spectra of the Ibu containing samples show the signals of Ibu but become wider, which would be due to a) the paramagnetic effect of cobalt atoms, b) the conformational distribution of the Ibu and/or the mobility of the Ibu in the solids and/or the mobility of the amorphous solids themselves.^{14a}



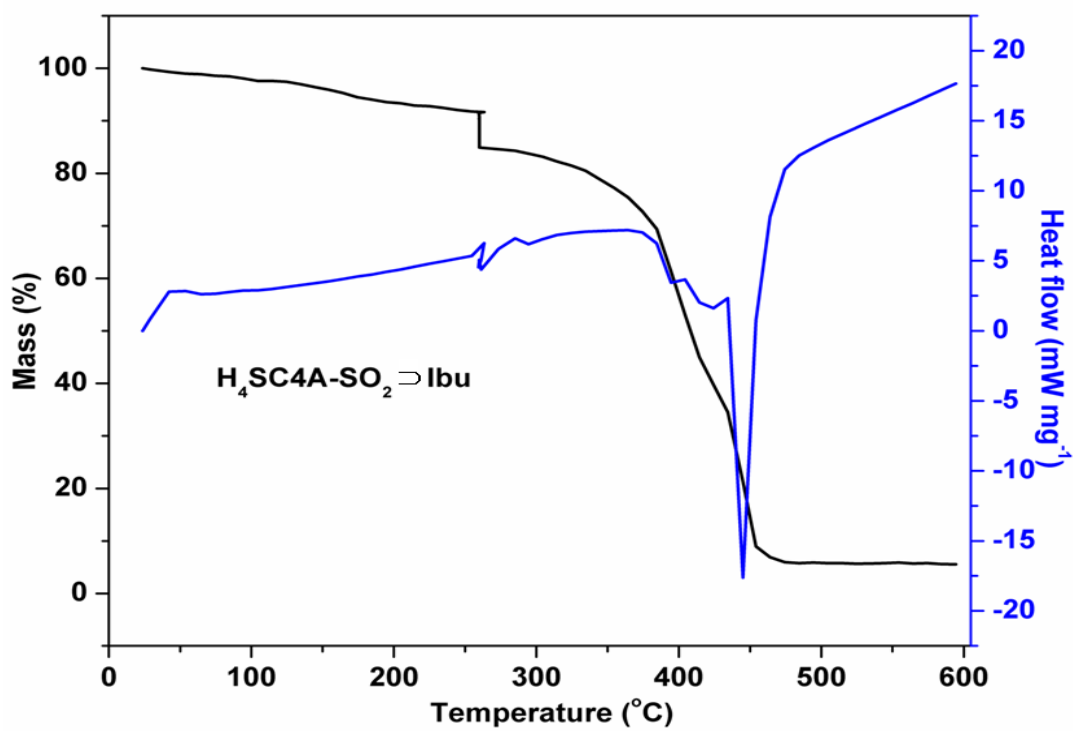
13. Fig. S12. TGA-DSC curves for **CIAC-114**. The samples were taken out from the mother liquor and washed with methanol. The apparent weight loss in temperature range from 27 °C to 200 °C can be attributed to the loss of solvated DMA molecules. According to the data, the calculated formula is $[(C_2H_5)_3NH]_6\{[Co_4(SC_4A-SO_2)(OH)]_6(BBB)_8\} \cdot 267(DMA)$, which shows more DMA molecules than that from the SQUEEZE results.



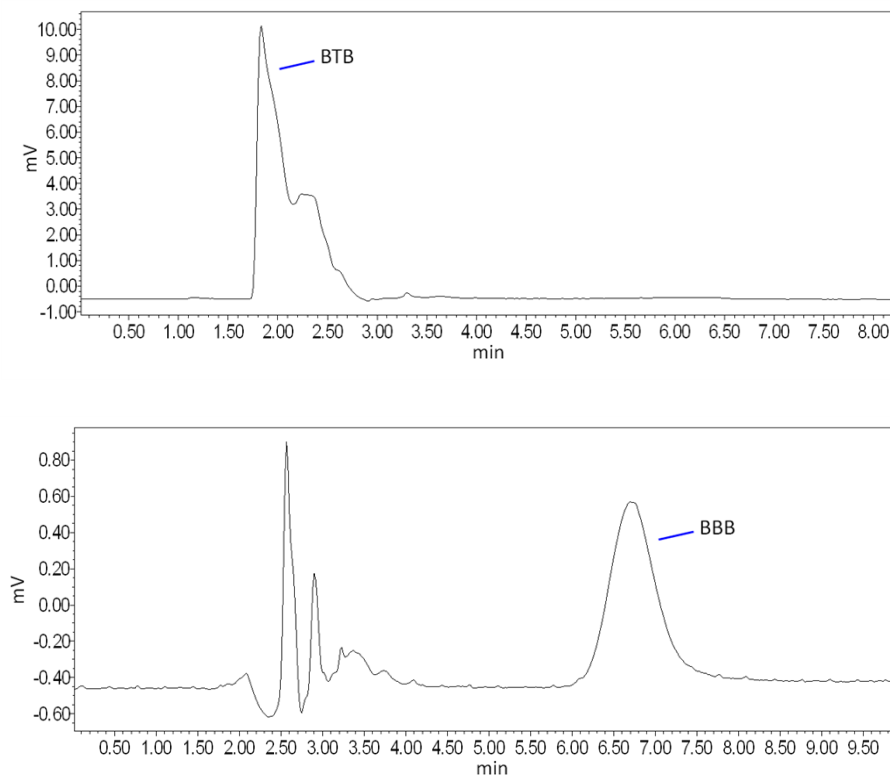
14. Fig. S13. TGA-DSC curves for **CIAC-106** to Ibu.



15. Fig. S14. TGA-DSC curves for CIAC-114 \rightarrow Ibu.



16. Fig. S15. TGA-DSC curves for H₄SC4A-SO₂ \rightarrow Ibu.



17. Fig. S16. Chromatograms for the samples of **CIAC-106** (upper) and **CIAC-114** (down) after immersed in PBS buffer solution for 22 hours.

After the solids of the cage compounds **CIAC-106** and **CIAC-114** were immersed in the PBS buffer solution for 22 hours, BTB and BBB were detected in the buffer solution by HPLC, which indicates that the cage structures are disassembled. So it is obvious that the Ibu release from the loaded samples is accompanied by the disassembly of the cage structures.